Impact of historical land cover changes on land surface characteristics over the Indian region using the Land Information System.

vibin jose (vibinjose20@gmail.com)
Indian Institute of Space Science and Technology
Anantharaman Chandrasekar
Indian Institute of Space Science and Technology
Suraj Reddy
ISRO Hyderabad: National Remote Sensing Centre

Research Article

Keywords: LSM, Noah, IMD, Land Information System (LIS)

Posted Date: May 10th, 2022

DOI: https://doi.org/10.21203/rs.3.rs-913048/v2

Climate Dynamics manuscript No.
(will be inserted by the editor)

Impact of historical land cover changes on land surface characteristics over the Indian region using the Land Information System

Vibin Jose[1] · **Anantharaman Chandrasekar**[1*] · **Suraj Reddy**[2]

Received: date / Accepted: date

Abstract The present study has employed a regional Land Surface Model (LSM) to investigate the impact of historical land cover changes on land surface characteristics over the Indian subcontinent for the period of 1930-2013. Four simulations that include a control run and three experiment runs are performed with the Noah 3.6 LSM within the Land Information System (LIS). The control run is performed with a MODIS-IGBP land cover map, while the three experimental runs are performed with three different potential land cover maps for the years 1930, 1975, and 2013. The potential land cover maps for the above three simulations are developed by blending the MODIS-IGBP data set with the fractional forest cover data set; the latter data is available for the years 1930, 1975, and 2013. Results indicate that the historical land cover change (1930 to 2013) has reduced the annual mean of latent heat flux and net surface heat flux over the Indian domain by -24.74 W/m^2 and -14.18 W/m^2 respectively, while the sensible heat flux and the soil temperature has increased by 4.97 W/m^2 and 2.78 K. The annual mean change in latent heat flux, sensible heat flux, and soil temperature demonstrate that the largest changes occur when the land cover changes from forest to urban land as compared to forest to cropland, forest to grassland and forest to open shrubland. The annual mean change in latent heat flux is moderately large for the land cover change from forest to open shrubland when compared to forest to grassland and forest to cropland. The above is attributed to the effects of evapotranspiration, which has high values for the cropland followed by grassland and open shrubland. Furthermore, the triple collocation method is employed to assess the impact of historical land cover change on soil moisture. Results indicate that the triple collocation method effectively demonstrates the impact of land cover change on soil moisture.

Keywords LSM · Noah · IMD · Land Information System (LIS)

*Corresponding Author:Anantharaman Chandrasekar

E-mail: chandra@iist.ac.in

[1] Department of Earth and Space Sciences, Indian Institute of Space Science and Technology, Valiamala P.O., Thiruvananthapuram - 695 547 Kerala, India

[2] National Remote Sensing Centre, Indian Space Research Organization, Hyderabad, Telangana, India

1 Introduction

The historical land surface changes that manifest over a country, typically occur through activities that are either (i) natural, (ii) anthropogenic or (iii) a combination of both. Deforestation refers to the depletion in forest areas across the world that are lost predominantly due to human activities such as (i) development of agricultural croplands, (ii) construction of urban infrastructure, and (iii) mining activities and increased urbanization. Natural forest fires, floods and diseases caused by parasites account primarily for the natural causes of deforestation. Deforestation that are caused by human activities have gained ascendancy since 1960s and their effects have accelerated in the last sixty years. Human activities are considered to be primarily responsible for deforestation globally with expansion of agricultural activity accounting for nearly 80% of the global forest cover loss. Construction of urban infrastructure (15%) and mining activities together with increased urbanization (5%) are the other human factors that are responsible for loss of forest cover worldwide. Deforestation not only impacts the atmospheric circulation (Dong et al., 2019; Deng et al., 2013; Dirmeyer et al., 2010) but also affects natural ecosystem, biodiversity and climate. Land cover changes are known to impact the climate through changes in surface albedo, sensible and latent heat fluxes, soil moisture, and soil temperature (Pitman, 2003; Pielke et al., 1998). Anyanwu (2015) and Tyagi et al. (2013) in their studies found that dense forest have higher soil moisture (SM) content as compared to degraded forest due to higher infiltration, dense roots, and higher organic content under dense forest. Earlier studies that have investigated the impact of deforestation have shown that strong cooling over the mid-latitude region is obtained (Betts, 2001; Betts et al., 2007; Hansen et al., 2005; Kvalevåg et al., 2010; Cherubini et al., 2018). The above result suggests that changes in albedo are a more dominant factor as compared to changes in evapotranspiration in determining the impact of deforestation over the mid-latitude regions (Betts, 2001; Hansen et al., 2005; Huang et al., 2020). However, over tropical regions, various studies have conclusively shown that the effects of evapotranspiration play a more dominant and important role as compared to changes in albedo, leading to surface warming over tropics (Bounoua et al., 2002; Bonan, 2008; Garratt, 1993; Feddema et al., 2005; Sampaio et al., 2007; Davin and de NOBLET, 2010; Lawrence and Chase, 2010; Pitman et al., 2012; Findell et al., 2006). Land cover changes are known to alter the characteristics of the land surface such as roughness length, leaf area index, stem area index, and surface albedo (Liu et al., 2015; Guo et al., 2016; Nair et al., 2011). Kvalevåg et al. (2010), show that impacts of deforestation leads to a reduction of (i) the rooting depth, (ii) stem area index, (iii) leaf area index, and (iv) roughness length, respectively. The reduction in the values of leaf area index, surface roughness, and vegetation cover contribute to lower rates of evapotranspiration (Pitman, 2003; Liu et al., 2019; Peng et al., 2014; Bright et al., 2017).

It is generally a well-accepted fact that as the surface albedo increases (with decreased forest cover), more solar radiation is reflected by the surface and the net effect will be surface cooling. Also, it is known that the reduced roughness length (with decreased forests) can contribute to reduced latent and sensible heat fluxes that results in surface warming (Liu et al., 2014). Furthermore the deep rooted forest vegetation that can access deep soil layers results in an increase in transpiration and latent heat flux and hence consequently to a decrease in sensible heat flux (from surface energy budget), as compared to a crop land or pasture region (Pielke et al., 2011).

Several earlier studies have investigated the impact of historical land surface change on climate by preparing the historical land cover maps. Chase et al. (2000) studied the impact of historical land cover change on climate using NCAR Community Climate Model 3 (CCM3) model. The study generated a natural vegetation map and an updated current vegetation map for the simulations, in which the updated current vegetation map is prepared by selecting regions, where the maximum leaf area index difference between the current and natural vegetation is more than one. In keeping with the standard land surface model vegetation, the above regions are represented by one of the three agricultural lands based on the maximum leaf area index difference, vegetation type in the standard Community Climate Model (CCM) data set, and latitude. The natural vegetation is prepared using the standard CCM data set, and assigned the agricultural areas with the appropriate standard vegetation types in the CCM data set. This is done by identifying the specific vegetation types with estimated potential maximum leaf area index values, latitude, and adjacent vegetation types. Kvalevåg et al. (2010) investigated the climate response caused by the land use change using global climate model. The study prepared the pre-agricultural data set using Ramankutty and Foley (1999) global vegetation cover data. The cropland plant functional type (PFT) in the present vegetation data set in Community Land Model 3.5 (CLM3.5) is replaced by the appropriate plant fuctional type from the Ramankutty and Foley (1999) data set. All biomes in the Ramankutty and Foley (1999) data set do not have appropriate PFTs used in the CLM3.5. If the biomes in the Ramankutty and Foley (1999) data set do not have appropriate PFT in the current CLM3.5, they use the PFT that is already there over the same region. Oleson et al. (2004) investigated the impacts of land use change on North American climate. The study prepared the natural vegetation data set by blending Ramankutty and Foley (1999) natural data set and CLM2 satellite-derived modern vegetation data set. The above is accomplished by eliminating the fraction of crop covered area from each grid cell of CLM2 satellite-derived modern vegetation data and these vacant areas of grid cells are filled with the existing natural PFTs. If the existing natural vegetation is less than the half of the grid cell, then the natural vegetation is derived from the neighbouring grid cells. The present study had also adopted a similar strategy and generated the historical land cover maps by blending the fractional forest cover data with MODIS-IGBP (Friedl et al., 2002) data set. In this study, the vegetation types for the potential historical data sets are generated by taking the MODIS-IGBP data set as the reference data set. Additional and more detailed procedure steps for the preperation of potential land cover maps are given in Section 2.2.1. The albedo, soil texture, and greenness fraction for the potential land cover maps are generated by using the corresponding National Centers for Environmental Prediction (NCEP) data sets (more details are included in section 2.2.2).

Observational records indicate that there have been extensive changes in land cover over the past hundred years over the Indian region, which has directly or indirectly affected the resultant land surface states. The percentage of deforested area over the Indian region in the last nine decades (1930-2013) is estimated as 28.01% (Reddy et al., 2018). There are several studies addressing the impact of land use/land cover change on the Indian summer monsoon region (Niyogi et al., 2018, 2010; Dutta et al., 2009; Halder et al., 2016). Gogoi et al. (2019) investigated the effect of land use/land cover (LULC) change on the surface air temperature over the eastern state (Odisha) of India using observations and reanalysis products. The results of the aforementioned study indicate that the mean surface air temperature over the state of Odisha has increased by 0.3 °C during the period 1981 to 2010 and about 25 to 50 % of surface

air warming is closely related to land use/land cover change. Halder et al. (2016) studied the impact of LULC change on the surface air temperature over the Indian domain using high-resolution regional climate model during 1951 through 2005. Results show a warming effect on daily mean and extreme temperature by 1-1.2 °C over central India. However, over India, most of the aforementioned studies have focused on the impacts of LULC on India summer monsoon rainfall and surface air temperature; with very little emphasis on the impact of LULC changes on the surface energy fluxes, soil moisture and soil temperature, respectively. In order to address the above objective, the present study, investigates the impact of historical land cover changes over the Indian region for a 83 year period on the land surface characteristics such as (i) surface energy fluxes (latent and sensible heat flux), (ii) soil temperature (ST), and (iii) soil moisture using the Noah land surface model (LSM).

In the following section, descriptions of the Model, data, and methodology are provided. While Section 3, describes the Experimental design. the Results and discussion are provided in section 4, Section 5 brings out the broad conclusions of the study.

2 Model, data, and methodology

2.1 LIS (Land Information System) and LSM

LIS is a software framework developed by NASA Goddard Space Flight Center for land surface modeling and data assimilation (Kumar et al., 2006). This software includes several land surface models that can be run on global or regional domains with horizontal resolution as high as 1 km. LIS integrates parallel high performance computing and communications technologies with modern land surface modeling techniques and data assimilation routines.

The present study uses the LIS software framework for running the Noah 3.6 land surface model (LSM) in offline mode (not coupled with atmospheric models) over the Indian subcontinent, that extends from 6.375 °N to 38.375 °N and 66.375 °E to 99.875 °E with a spatial resolution of 4 km. The development of Noah LSM (Chen et al., 1996) is initiated by the four agencies, National Center for Atmospheric Research, Oregon State University, U.S. Air Force, and National Centers for Environmental Prediction's Office of Hydrology. The Noah LSM may be used either as uncoupled mode or embedded within an atmospheric model. The Noah LSM calculates soil moisture and soil temperature over four soil depths (0-0.1 m, 0.10-0.30 m, 0.30-0.60 m, 0.60-1 m). The Noah LSM requires the following inputs to simulate the land surface processes over time, (i) land surface parameters, which include land cover data, soil texture, surface albedo, and greenness fraction etc, (ii) atmospheric forcings that include surface meteorology, surface radiation components and precipitation, and (iii) initial land surface state.

2.2 Land surface parameter data sets

The present study uses the Moderate Resolution Imaging Spectroradiometer-International Geosphere-Biosphere Programme (MODIS-IGBP) land cover data and temporal fractional forest cover data over the Indian region. The MODIS-IGBP data has twenty land cover classes at a spatial resolution of 0.9 km (30 s) (Friedl et al., 2002). The fractional forest cover data is developed using multi-source and multi-temporal

remote sensing data for the years 1930, 1975 and 2013 by Reddy et al. (2018) and is made available through NICES portal of National Remote Sensing Centre, Indian Space Research Organization (`https://bhuvan-app3.nrsc.gov.in/data/download/index.php?c=p&s=NI&g=OS`). The fractional forest cover information was primarily based on classification of forest cover and subsequent spatial grid-analysis at 5km scales. For this study, we have used an identical grid surface as of MODIS-IGBP land cover data so as to overlay and generate potential land-cover maps (for more details refer Section 2.2.1). The forest cover for the year 1930 is generated using the topographical maps (1:250,000 scale) prepared by US ARMY services during the years 1920 - 1940. The 1975 forest cover information is obtained using Landsat Multi-spectral Scanner (MSS) data from 1972-1977 over Indian region. Indian Remote Sensing (IRS) satellite Resourcesat-2 AWiFS data was used to generate 2013 forest mask. All the remote sensing data sets are subjected to noise removal and precise geometric corrections before classification of forest cover. The atmospheric corrections were also performed using the top-of-atmosphere reflectance algorithms. The interpretation of remote-sensing data sets was carried out using a hybrid approach of digital image classification and visual interpretation to minimize the changes associated with sensor differences as well as with phenological, atmospheric and environmental variability. Multi-source data sets corresponding to 1920-1940, 1972-1977, and 2013-2014 are being referred to as 1930, 1975, and 2013 periods respectively. The soil texture map data has been taken from State Soil Geographic-Food and Agriculture Organization (STATSGO-FAO) (Miller and White, 1998) (Reynolds et al., 2000) soil texture map. It has 16 soil texture classes with a spatial resolution of 0.9 km (30 s). The elevation data is provided by the Shuttle Radar Topography Mission (SRTM)(van Zyl, 2001) data. The greenness fraction (Gutman and Ignatov, 1998), slope type (Zobler and for Space Studies, 1986), and albedo (Csiszar and Gutman, 1999) data sets are taken from National Centers for Environmental Prediction (NCEP) data sets. International Satellite Land Surface Climatology Project 1 (ISLSCP1)(Sellers et al., 1988) bottom temperature data sets are utilized for the bottom temperature data for the present study. The above data sets are available at the LIS data portal (`https://portal.nccs.nasa.gov/lisdata_pub/`). Figure 1 shows the regions where the historical land cover changes with significant depletion in forest cover have manifested over the Indian domain between the years 1930 and 2013. It is clear from Figure 1 that significant depletion in forest cover over the Indian domain between the years 1930 and 2013 is restricted to regions that represent some areas of (i) North India, (ii) Central India, (iii) Northeast India, and (iv) Western ghats.

2.2.1 Preparation of potential land cover map

Since the fractional forest cover information is void of any classification information on other land-use land cover classes, we have generated potential land cover maps by blending MODIS-IGBP (Friedl et al., 2002) land cover information with the temporal fractional forest cover data. The land cover types are fixed to a single land cover class for each grid point in the Noah model, while the preparation of potential land cover is performed by using an appropriate cutoff value of 0.5. If the fraction of forest cover in a grid point is above the cutoff value of 0.5, the corresponding grid point in the potential land cover map is represented by the adjacent forest vegetation class of MODIS-IGBP. The cutoff value was appropriately chosen in such a way that it satisfied the following requirement; number of grid points that manifested

change between 1930 potential land cover and 2013 potential land cover are reflect the actual change between the 1930 and 2013 fractional forest cover data. The preparation of potential land cover map is performed in the following two steps. In the first step, the potential land cover map of year 2013 is generated by modifying the MODIS-IGBP non-forest vegetation (such as croplands, urban and built-up, cropland mosaics, bare soil and rocks) to forest vegetation class, if the corresponding grid point in the fractional forest cover data has value above 0.5. Also, the forest cover class information for such grids with only fractional forest cover data is fashioned on the assumption that it would be similar to the adjacent forest vegetation class. Applying the aforesaid idea, each forest vegetation grid point in the MODIS-IGBP land cover map is replaced by nearby non-forest vegetation, provided the corresponding grid point in the fractional forest cover data has a value below 0.5. In the second step, the potential land-cover map of 2013 is used in the generation of potential land cover map for 1975 by replacing the non-forest vegetation of each grid point in the 2013 layer to nearby forest vegetation by checking the corresponding grid in the 1975 fractional forest cover data and ascertaining that the fractional forest cover data has a value above 0.5 at that grid point. Additionally, the potential cover data for the year 1930 (refer Figure 2) is prepared by changing 1975 potential cover data using the 1930 fraction forest cover data by following the aforementioned methodology.

2.2.2 Modified soil texture, albedo, and greenness fraction data sets

The land surface parameters such as soil texture, albedo, greenness fraction are also suitably modified every time the potential land cover map is generated. The present study has obtained the soil texture data from the State Soil Geographic-Food and Agriculture Organization (STATSGO-FAO) soil texture map. For each MODIS-IGBP vegetation has more than one STATSGO-FAO soil texture type over the Indian domain. For example, the Evergreen broad leaf forest vegetation class of MODIS-IGBP has four different soil texture (Clay loam, Sandy clay loam, Loam, and Sandy loam) types over the Indian domain in which the "clay loam" soil texture type is dominant compared to the other three soil texture types. The soil texture at a grid point corresponding to the modified vegetation is replaced by the dominant soil texture that corresponds to the appropriate modified vegetation class of MODIS-IGBP data over the Indian domain. For example, assume that a grid point corresponding to the modified vegetation is Evergreen broad leaf forest as land cover. Then the corresponding dominant soil texture for the Evergreen broad leaf forest class over the Indian domain is identified and let it be "clay loam". The soil texture at the identified grid point over which the landcover is being changed is then modified to "clay loam" type.

Kvalevåg et al. (2010) investigated the impact of land cover change on climate using global climate model. The above study utilized the present day land cover data from MODIS-IGBP data as well as the pre-agriculture land cover data prepared using Ramankutty and Foley potential (Ramankutty and Foley, 1999) vegetation data set. For calculating the surface albedo for the pre-agricultural conditions, Kvalevåg et al. (2010)calculated a surface albedo for each vegetation class in the present day MODIS-IGBP data set by averaging albedo in all grid cells for each MODIS-IGBP vegetation class, where the fractional vegetation class is more than 95 %. The present study had also adopted a similarly strategy for calculating the surface albedo values and greenness fraction values for the potential lancover maps. Hence, the present study has calculated a the monthly albedo and Greenness fraction of each vegetation class of

MODIS-IGBP by taking the mid-value of each monthly data of the above land surface parameters over the range of values corresponding to each vegetation class that is observed over the Indian domain. For example, the Evergreen broad leaf forest vegetation class has a range of values for albedo and greenness fraction for the month January, and the mid-values for the albedo and greenness fractions are 0.15 and 0.4 for the month January. Assume that the modified vegetation class is Evergreen broad leaf forest, then the corresponding albedo and greenness fraction values for the above vegetation class for January is replaced by 0.15 and 0.4.

2.2.3 Assumptions of the study.

The following assumptions have been made for the Noah LSM in LIS, preperation of potential landcover map and the correponding changes in albedo, grenness fraction, and soil texture.

1. In a grid point if the fractional forest cover data has value above or equal to 0.5, then the corresponding grid point in the potential land cover map is considered as a forest vegetation class. Similarly, if the fractional forest data has value below 0.5, then the corresponding grid point in the potential land cover map is considered as non forest vegetation class.
2. The forest vegeatation class at a grid point corresponding to the modified vegetation data in the potential landcover map is represented by the adjacent forest vegetation class of MODIS-IGBP land cover data. Furthermore, the non forest vegetation class is also determined in a similar manner for the presnt study.
3. The soil texture type for the modified vegetation class in the potential land cover map is represented by the dominant STATSGO-FAO soil texture type of the corresponding MODIS-IGBP vegetation class.
4. The monthly albedo for the modified vegetation class in the potential land cover map is determined by calculating the mid-value of the range of albedo values in the respective MODIS-IGBP vegetation class corresponding to each month. Similarly, the greenness fraction values also determined for the presnt study.
5. The present study forced the Noah LSM with IMD gridded rainfall data. Despite having a low temporal resolution, the IMD gridded rainfall data forced Noah LSM soil moisture output is closer to IMD in-situ data as compared to high resulution data set such as GPM, TRMM, and GDAS rainfall data set (Jose and Chandrasekar, 2021)
6. The land surface model employed in this study is the one dimensional Noah 3.6 LSM. The Noah MP (Multi-Parameterization) LSM has multiple parameterization options for the selected land-atmospheric processes as compared to Noah 3.6 LSM and hence one of the assumptions of the present study is that the effect of multi parameterization option effects are not considered.

2.3 Meteorological forcing data.

The meteorological forcing data are obtained from Global Data Assimilation System (GDAS) and Indian Meteorological Department (IMD) rainfall data. The NCEP GDAS Final (FNL) operational global analysis data (Rodell et al., 2004) is available with a spatial resolution of $0.25^\circ \times 0.25^\circ$ and operationally

at every six hours. The GDAS data has assimilated surface observations, aircraft reports, balloon data, radar observations, wind profiler data, and satellite observations into a gridded model space by employing a four-dimensional multivariate method. Jose and Chandrasekar (2021) assessed the impact of five different rainfall forcing (IMD griided rainfall, TRMM-TMPA, PERSIANN-CDR, GDAS, and GPM) on soil moisture using Noah land surface model within the LIS, over the Indian domain and found that the IMD gridded rainfall data forced Noah LSM output soil moisture shows better results compared to the other four rainfall forced soil moisture outputs. Hence, the present study used the IMD gridded rainfall data for forcing the Noah LSM. The IMD gridded rainfall data is prepared using daily rainfall records from a dense network of 6955 rain gauge stations over the Indian region (Pai et al., 2014). The high spatial resolution IMD gridded data set is developed by using an inverse distance weighted interpolation (IDW) scheme. The above data set is available as 24 hr accumulated rainfall data with a high spatial resolution of $0.25^\circ \times 0.25^\circ$

2.4 Triple collocation (TC) method.

The present study has evaluated the impact of land cover change on soil moisture estimate using triple collocation (TC) method. While the above method was proposed initially by Stoffelen (1998) for ocean studies, in subsequent years the TC method has been widely employed in soil moisture studies (Wu et al., 2020; Kolassa et al., 2017; Nair and Indu, 2019). The basic idea of TC method relies on the availabilty of three independent measurements of the same variable. The error covariance of these data sets are obtained by data collocation (Gruber et al., 2017; Wu et al., 2020). For the present study, TC based Extended Triple Collocation (ETC) method is adopted from McColl et al. (2014). To ensure that the assumptions of the TC method are applicable, the present study has utilized soil moisture estimates from MERRA (Modern-Era Retrospective analysis for Research and Applications) Land data and Global Land Data Assimilation System (GLDAS) Catchment Land Surface Model (CLSM), data set along with the 1930 potential land cover simulation soil moisture output as the triad of independent measurements on soil moisture. Furthermore, soil moisture data from MERRA, GLDAS and the 2013 potential land cover simulation soil moisture output constitute a second triad of independent measurements of soil moisture.

2.5 Model initialization

2.5.1 LIS spin up

Obtaining accurate land surface initialization in a LSM is critical for deriving the evolution of the land surface characteristics with time (Dirmeyer and Halder, 2016). Initial conditions for land surface models are obtained through spin up process (Rodell et al., 2005). The present study employed a common method for initializing the Noah LSM, by spinning up the LSM through several iterations repeatedly through a single year until the soil equilibrium is reachedCase and Peters-Lidard (2007).

Earlier studies have assessed the imapct of historical land cover change on climate, by comparing a simulation, where the land cover map is represented by the present day land cover map to a simulation

where the land cover map is represented by the historical land cover map (potential land cover) with the same meteorological forcings. Chase et al. (2000) investigated the impact of historical land cover change on climate in northern winter using global circulation model. The simulations with present land cover and the historical land cover maps are drived by the current climate as the boundary conditions. Mishra et al. (2010) studied the regional impact of land cover change on climate by running the variable infiltration capacity (VIC) land surface model offline. The study uses the same meteorological forcings for the simulations with (i) present land cover data, (ii) historical land cover data, and (iii) future projected land cover data for the year 2030. In the present study, all the four simulations are initialized by running the Noah LSM forced with the same atmospheric forcings for all simulations. Table.1 lists the summary of model and data utilized in this study. For obtaining the initial condition on 01 June 2013 00 UTC, the Noah LSM is integrated by assuming an initial soil moisture and soil temperature values as 0.15 m^3/m^3 and 298 K at all four layers and all grid cells on 01 June 2012 00 UTC. The Noah LSM is then integrated for an year till 01 June 2013 00 UTC (first loop). The Noah LSM is then integrated again for the above same period (2nd loop) by reassigning the initial values of land surface variables on 01 June 2012 00 UTC with 01 June 2013 00 UTC. The above step is repeated until the changes in the deepest layer (0.60-1 m) soil moisture differences between the successive loops is less than 5%.

3 Experimental design

The impact of historical land cover change on land surface characteristics over the Indian region is investigated using the Noah LSM with historical fractional forest cover maps over the Indian region. The present study conducted the control run and three experimental runs. In the control run (Ctl-run), the Noah LSM is forced with meteorological forcing data from GDAS and IMD (rainfall data) data and the land surface parameters such as land cover, soil texture, albedo, and greenness fraction are obtained from MODIS-IGBP land cover map, STATSGO-FAO soil texture map, and NCEP (albedo and greenness fraction) data sets respectively. The remaining three experimental runs are conducted by forcing the Noah LSM with the same land parameters and atmospheric forcings as that of the Ctl-run, except that the land cover map, albedo, soil texture, and greenness fraction data are different for the three simulations. For the three experimental runs, the land cover data sets are derived from MODIS-IGBP data using fractional forest cover maps of 2013, 1975 and 1930, respectively. The soil texture, albedo, and greenness fraction are also modified from the corresponding data sets (STATSGO-FAO, NCEP) for the three experimental runs. The experimental run, which uses the potential land cover map for 1930, 1975, and 2013 is hereafter identified as Exp1-run, Exp2-run, and Exp3-run respectively. The model runs, and the type of input data sets used in the model are given in Table 2.

All the four model LSM simulations are initiated from 01 June 2013 00 UTC and integrated for a period of one year over the Indian region that extends from 6.375 °N to 38.375 °N and 66.375 °E to 99.875 °E with 4km horizontal spatial resolution.

Table 1 Model and data used

Model used	Model resolution	Land parameters used	Meteorological forcing used (GDAS)	Precipitation data (resolution)
Noah 3.6	4 km	Potential land cover	Near surface air temperature	IMD (0.25 °×0.25 °)
		Modified soil texture	Near surface specific Humidity (kg/kg)	
		SRTM(Elevation)	Incident shortwave radiation ($\frac{W}{m^2}$)	
		Modified monthly albedo	Incident longwave radiation ($\frac{W}{m^2}$)	
		NCEP(Maximum snow albedo)	Near surface zonal wind ($\frac{m}{s}$)	
		NCEP(slope type)	Near surface meridional wind ($\frac{m}{s}$)	
		Modified Greeness fraction	Surface pressure (Pa)	
		ISLSCP1(Bottom temperature)	Rainfall rate ($\frac{kg}{m^2}$)	

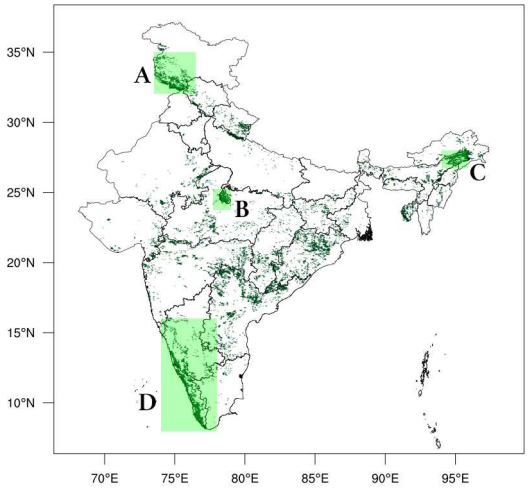

Fig. 1 The significant change in forest cover between the years 1930 and 2013 over the Indian domain. The rectangular shaded regions represent North India (A), Central India (B), Northeast India (C), and Western ghats (D), where the land cover changes are significant.

4 Results and Discussions

4.1 Validation of control run soil moisture output

Figure 3 shows the correlation and RMSE of EXP3 and control run (ctl-run) soil moisture output with GLEAM (Global land evaporation Amsterdam model) soil moisture data set for all seasons at 5 cm depth. The GLEAM is a group of algorithms used to estimate the soil moisture data from satellite data. The data is available globally at a horizontal resolution of 0.25 °. From Figure 3 it is clear that the ctl-run and EXP3 run soil moisture have positive correlation with the GLEAM soil moisture data set. The correlation of ctl-run has higher values compared to EXP3 for all seasons, while the RMSE is minimum for ctl-run output soil moisture. The correlation is maximum during monsoon and postmonsoon season compared to the other two seasons.

4.2 Impacts on land surface characteristics

The potential impact of land cover change on surface variables is substantial only over regions where the land cover changes are significant (Chase, 1999). For the present study, regions of significant land cover changes are selected (Western ghats, Central India, North India, and Northeast India) to analyze the impact of land cover changes on land surface characteristics (refer Figure 1). Since the change in

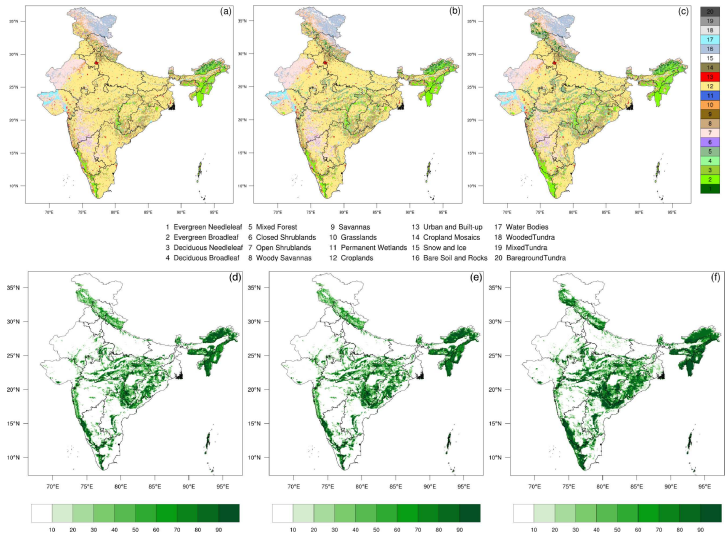

Fig. 2 The potential land cover map (a), (b), and (c) (top panel) and the fractional forest cover map (percentage) (d), (e), and (f) (bottom panel) for the years 2013, 1975, and 1930 respectively.

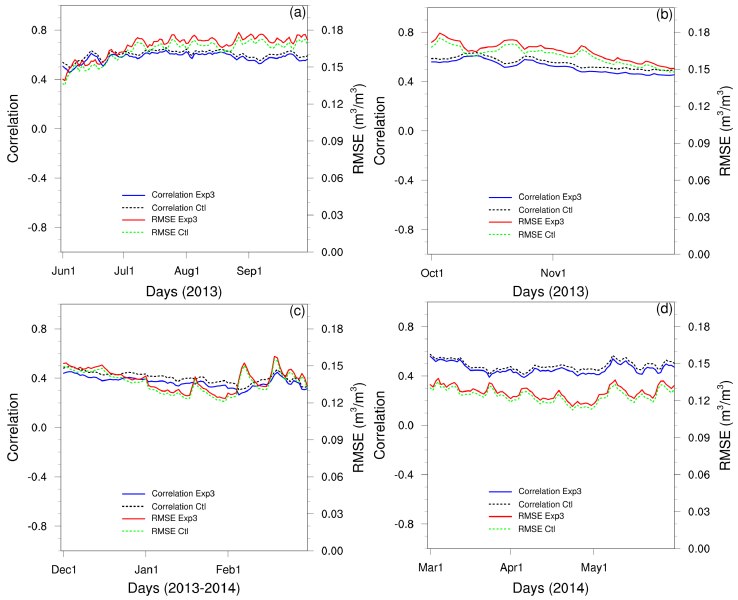

Fig. 3 Soil moisture RMSE and correlation of EXP3 run and control run (ctl-run) with GLEAM soil moisture data set at 5 cm depth for (a)Monsoon (b)post-monsoon (c)winter (d)pre-monsoon over the Indian domain.

fractional forest cover for the years 1975 and 2013 is not significant as compared to the change in fractional forest cover between the years 1930 and 2013 (refer Figure 2), the land surface characteristics are similar for the Exp2-run and Exp3-run over India for all seasons. Although Figure 4 and Figures 8 to 11 depict the model output from all three experimental runs, considering the closeness of the results of Exp2-run and Exp3-run, the discussion of the results would be confined mostly to the simulation of Exp1-run and Exp3-run, respectively.

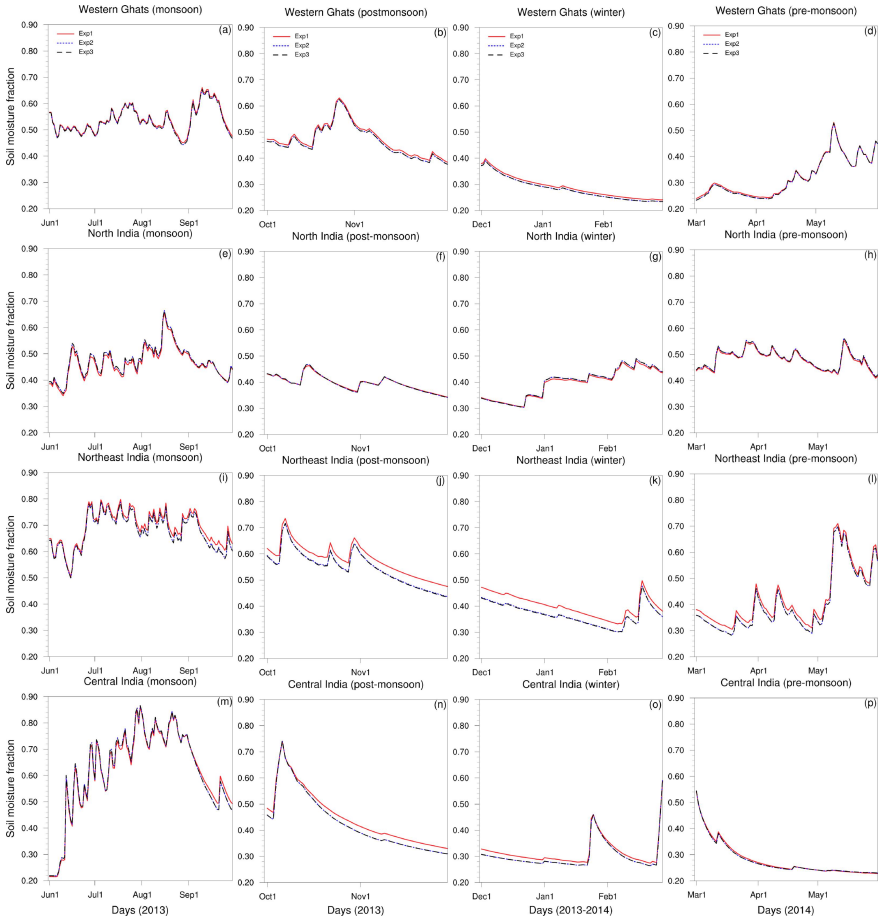

Fig. 4 Time series of daily mean soil moisture fraction spatially averaged over Central India, North India, Northeast India, and Western ghats at 5 cm depth for different seasons for all three experimental runs.

4.2.1 Impacts on soil moisture and soil temperature

Land use/land cover plays a crucial role in regulating the spatial and temporal variation of soil moisture (SM) by influencing the following processes such as surface runoff, infiltration, radiation balance, surface albedo and evapotranspiration (Niu et al., 2015). Figure 4 shows the time series of daily mean soil moisture fraction (SMF)(Scaled using soil moisture porosity) spatially averaged over Central India, North India, Northeast India, and Western ghats at 5 cm depth for different seasons and for all the three experiment run simulations. The spatial averaged SMF over a particular region, say, Central India would average the SMF over all the grid points that encompass that region, i.e., over Central India. All regions show high SMF values during the monsoon season. This is attributed to the fact that India, as a whole, receives 85 % of annual rainfall during the monsoon season. From figure 4, it is clear that the SMF estimates from the Exp1-run show a noticeably higher value than that of Exp3-run for all regions and all seasons, except for the North Indian region, where the Exp1-run SMF values are lower as compared to the other two simulations. The explanation for the above is that the modified soil texture for Exp1-run over the North Indian region has low field capacity values as compared to the Exp3-run. From Figure 6, it is evident that over the North Indian region, the soil texture classified as Clay (Field capacity value (0.38)) and Clay loam (Field capacity value (0.362)) for the Exp3-run are changed to Loamy soil texture (Field capacity value (0.335)) for the Exp1-run. The Clay and Clay loam soils have a higher field capacity

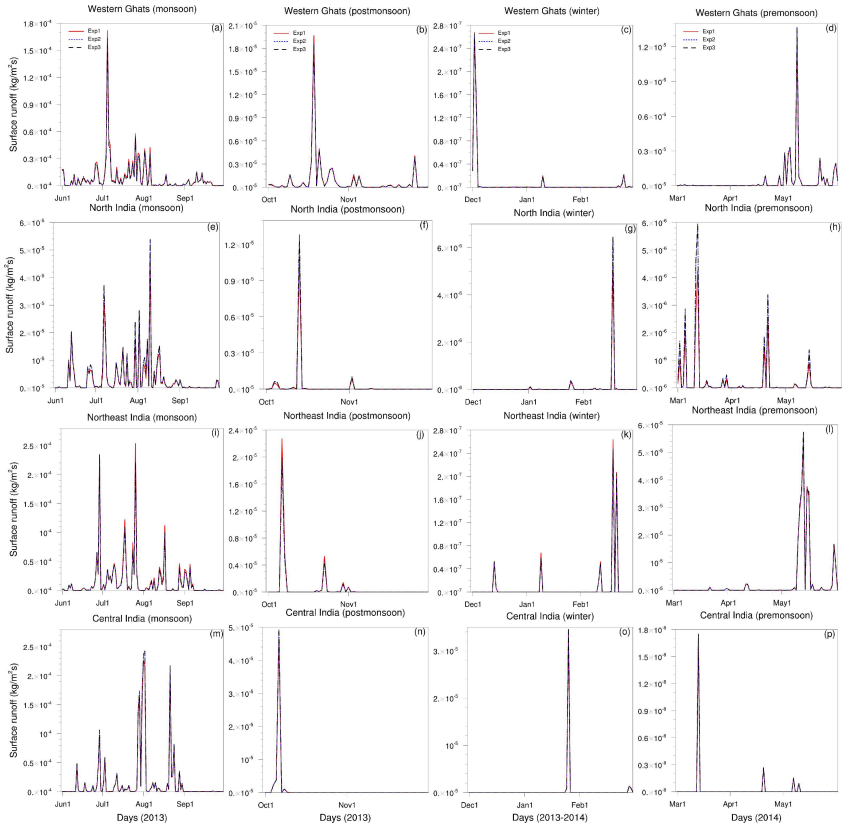

Fig. 5 Time series of daily mean surface run off spatially averaged over Central India, North India, Northeast India, and Western ghats for different seasons for all three experimental runs.

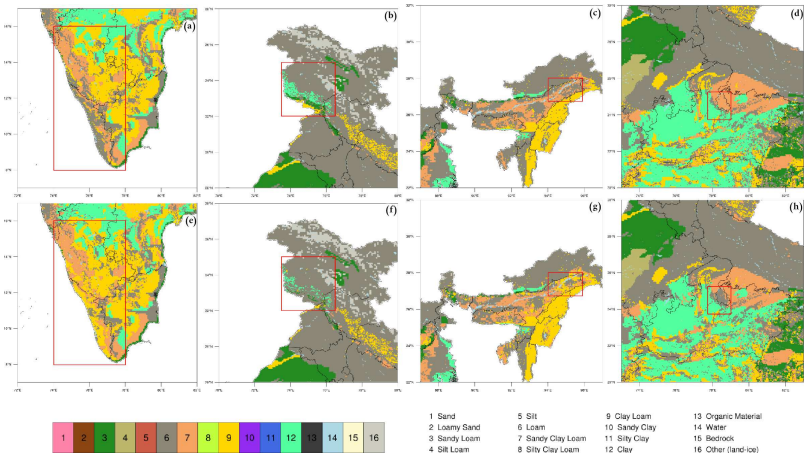

Fig. 6 Modified soil texture map derived from STATSGO-FAO soil texture map for the years 2013 (top panel) and 1930 (bottom panel) over Western ghats (a), North India (b), Northeast India (c), and Central India (d).

and lower soil conductivity values as compared to Loamy soil; thus, soil water drains more rapidly in the Loamy soil layers as sub-surface runoff, which reduces the SM over the North Indian region. Figure 5 depicts the time series of daily mean surface run off spatially averaged over Central India, Northeast India, North India, and Western ghats for different seasons. From Figure 5, it is clear that over North India the surface run off is lower for the EXP1 run compared to EXP3. The above feature is observed for North Indian region over all the four seasons. Over the Western Ghats, for Exp1-run, the modified soil texture is classified as Clay Loam (refer to Figure 6); while in Exp3-run, the modified soil texture is

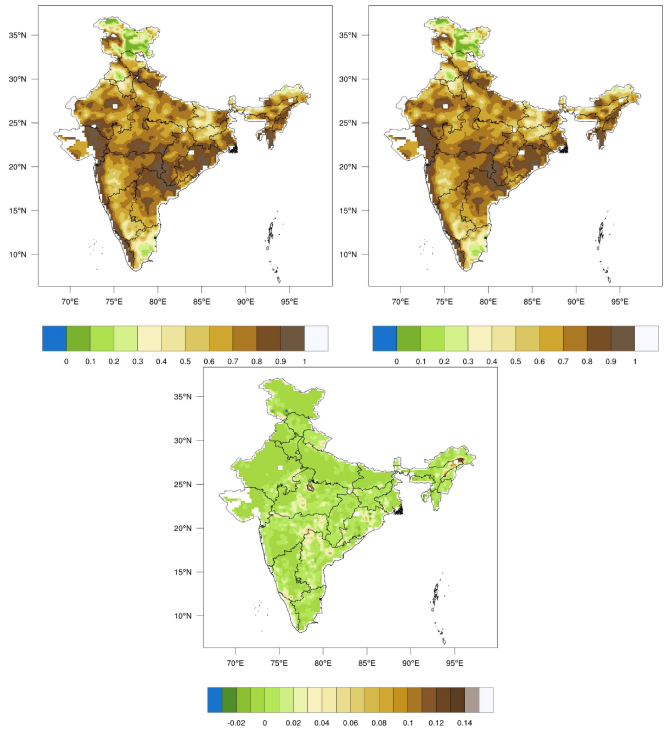

Fig. 7 Squared correlation coefficient obtained using TC method for (a) Exp3 run and (b) Exp1 run soil moisture, (c) depicts the change in squared correlation coefficient of Exp1 and Exp3.

classified as Loam. The SMF estimates in the Exp1-run are higher than the Exp3-run over the Western ghats for all the four seasons. The Loam soil texture is associated with coarser particles as compared to Clay Loam. It is well known that the soil conductivity increases with the increase of coarser particle size. Soil electrical conductivity is a measure of the amount of salts in the soil. It is known that soils having excess salt content hinders plant growth and hence such soil with high soil conductivity are associated with arid and semi-arid environments that have lower SMF values. The above is also clear from Figure 5, that the surface run off over the Western ghats has higher values for EXP1 as compared to EXP3 for all the seasons. The aforementioned argument explains the increase in SMF for the Exp1-run over the Western ghats as compared to Exp3-run for all the four seasons. Similarly, over Central India and Northeast India, Exp1-run has higher SMF as compared to Exp3-run for all the four seasons. The change in SMF estimates between Exp1-run and Exp3-run is higher over Central India and Northeast India as compared to Western ghats for all the four seasons. The percentage of grid points over which the land cover has changed between the years 2013 and 1930 over Western Ghats, Northeast India, North India, and Central India are 10%, 34%, 19%, and 21% respectively. Since the percentage of grid points in which the land cover change is large over Northeast India (34%) and Central India (21%), the change in fractional soil moisture is also large over the above regions as compared to the other two regions. During the monsoon season the rainfall is excessive over all the four regions as compared to post monsoon and winter seasons. Also, the pre-monsoon season is characterized by convective type of rainfall over India that also has marked rainfall. The above would correspond to high evapotranspiration during the monsoon and pre-monsoon seasons for both the years 1930 and 2013. However, the results of the study indicate that the change in fractional soil moisture is low during the monsoon and pre monsoon season

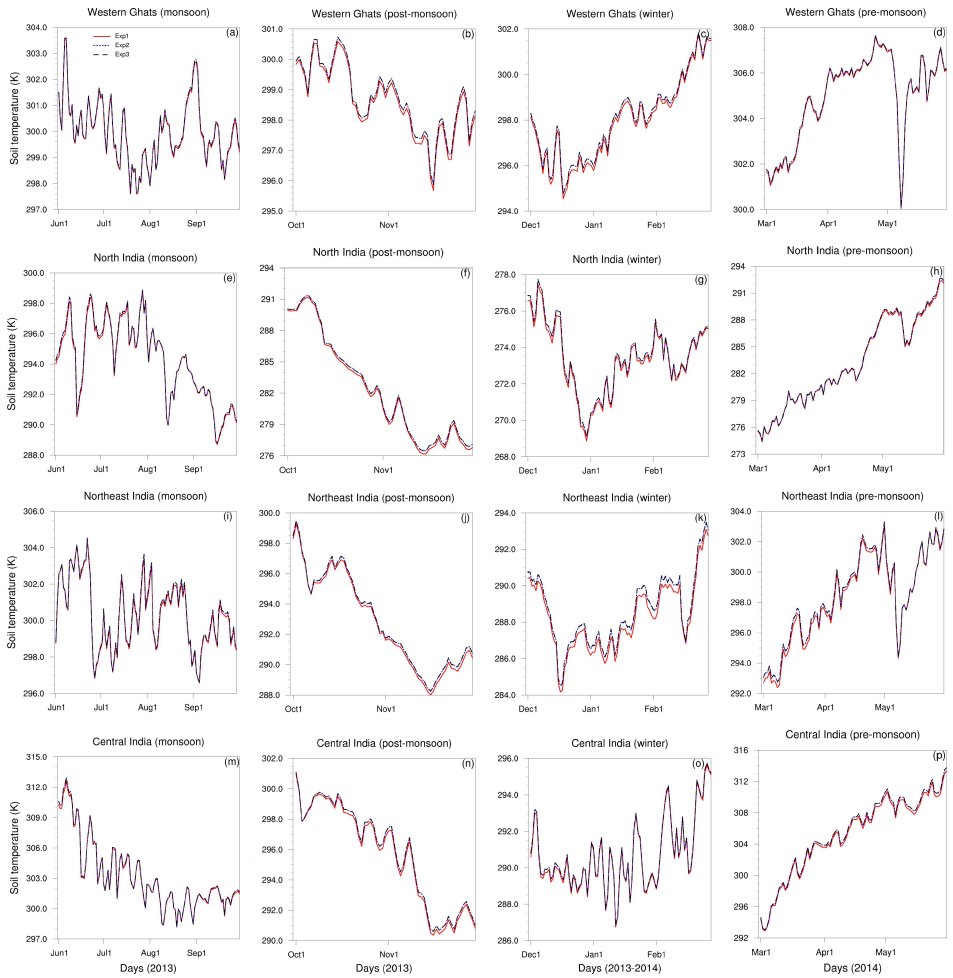

Fig. 8 Time series of daily mean soil temperature spatially averaged over Central India, North India, Northeast India, and Western ghats at 5 cm depth for different seasons for all three experimental runs.

between the years 1930 and 2013. The above is attributed to the fact that the rainfall is excessive and marked during the above seasons as compared to post monsoon and winter seasons. In addition, since the soil pores are recharged regularly by rainfall, the change in evapotranspiration between the years 2013 and 1930 is minimal during the monsoon and post monsoon season. From Figure 4, it is clear that during dry seasons the SMF estimates are higher for the Exp1-run as compared to Exp3-run, except for the North Indian region.

Furthermore, the impact of land cover change on SM is evaluated using triple collocation (TC) method. Two groups of triplets are employed for the TC analysis. The SM obtained from GLDAS CLSM and MERRA Land data are both utilized as two independent measurements kept same for both triplets while the third independent measurement is the SM in each of the two triplet group, i.e., SM from Exp1 and Exp3 SM simulations. The TC analysis is performed for the entire study period and the squared correlation coefficients are obtained by adopting McColl et al. (2014) approach. Figures 7a and 7b show the squared correlation coefficient of Exp1 and Exp3 SM estimate, while Figure 7c depicts the change in squared correlation coefficient of Exp1 and Exp3 SM estimate. From Figures 7c it is clear that the change in squared correlation coefficient is maximum over Central India and Northeast India with values ranging from 0.12 to 0.14, while the change in squared correlation coefficient is less than 0.02

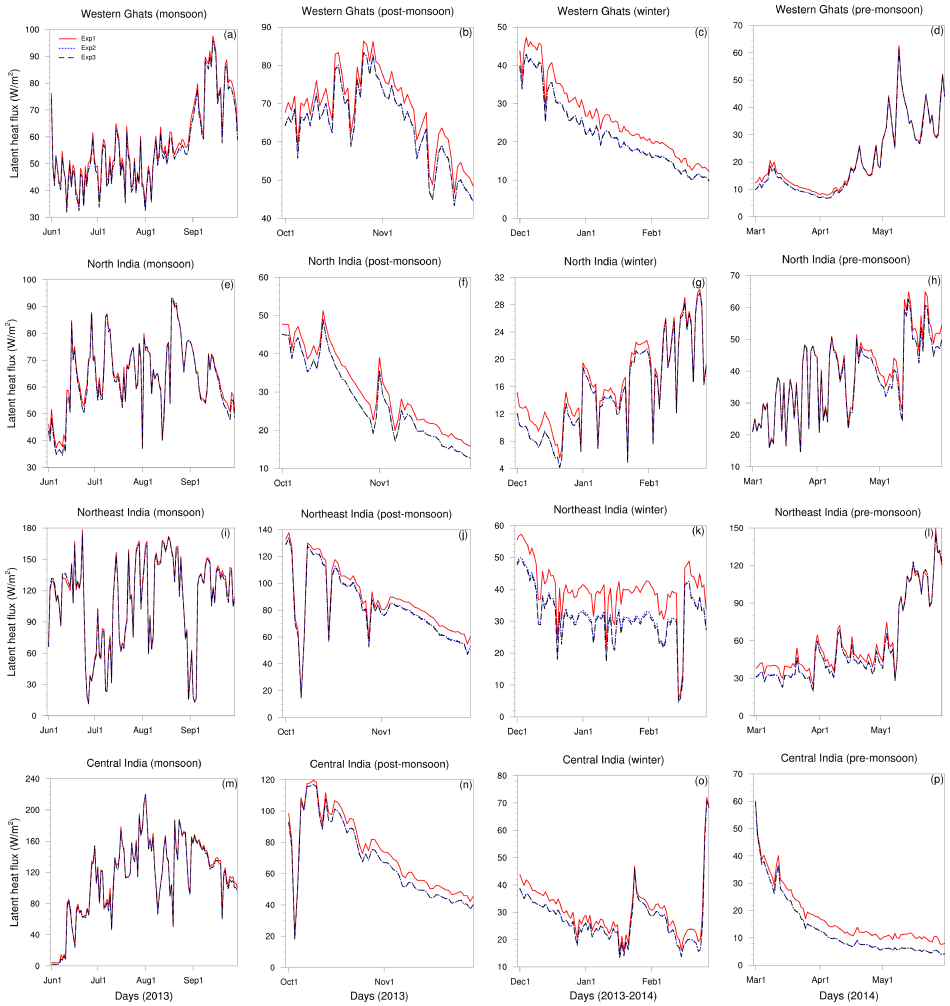

Fig. 9 Time series of daily mean latent heat flux spatially averaged over Central India, North India, Northeast India, and Western ghats for different seasons for all three experimental runs.

over Western ghats and North India. The change in squared correlation coefficient with values ranging from 0.03 to 0.06 over the regions of Telegana, Maharashtra, Madhya pradesh, and Uttarakhand where the land cover changes are also significant (refer to Figure 1). The above results indicate that the TC analysis has effectively captured the impact of land cover change on SM.

The daily cycle of soil temperature primarily depends on the position of the sun and air temperature. However, factors such as land cover and soil moisture also play an important role in the daily soil temperature (ST) cycle. It is known that the high SM content and the effect of land cover shading will result in a decrease in the soil temperature. Additionally, the low SM values will contribute to increased soil temperature values; the aforementioned effect will however be weaker below forest canopies than grasslands (Lozano-Parra et al., 2018). Figure 8 shows the time series of daily mean soil temperature spatially averaged over Central India, North India, Northeast India, and Western ghats at 5 cm depth for different seasons and for all the three experimental runs. From Figure 8, it is clear that the soil temperature (ST) attains its lowest value during the winter season and its highest value during the end of the pre-monsoon season. The aforementioned observation can be explained due to the low solar radiation during winter season while the highest ST value is attained during the season that has dominant

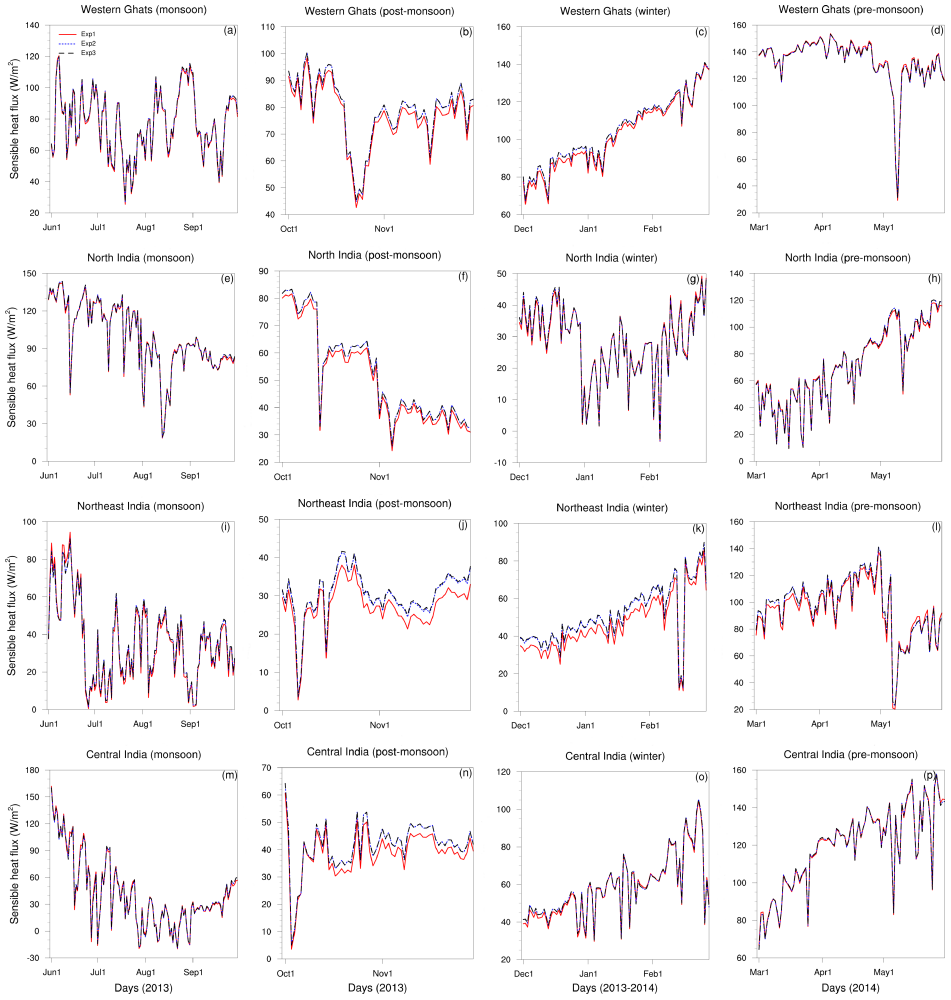

Fig. 10 Time series of daily mean sensible heat flux spatially averaged over Central India, North India, Northeast India, and Western ghats for different seasons for all three experimental runs.

solar radiation accompanied by very limited cloud cover. The results of Exp1-run shows a decrease in soil temperature as compared to Exp3-run for all regions and all seasons (refer Figure 8). It is known that the removal of trees (reduced forest cover in Exp3-run) decreases the shading of the surface which will have a warming effect on the land surface contributing to a slight increase in the soil temperature in Exp3-run. Additionally, the decrease in evaporation rate for the Exp3-run due to low soil moisture values (refer Figure 4) provides additional available energy at the surface leading to an increase in soil temperature values.

4.3 Impacts on surface fluxes

Figures 9 and 10 show the time series of daily mean latent heat and sensible heat flux (LHF and SHF) spatially averaged over Central India, North India, Northeast India, and Western ghats for different seasons and for all the three experimental run simulations. The LHF during winter season is lower for all four regions as compared to the other three seasons for all experimental simulations, indicating lower evapotranspiration due to reduced soil moisture during the winter season. For all four regions, the Exp1-run shows increased LHF values as compared to the Exp3-run for all the seasons. This is due to the

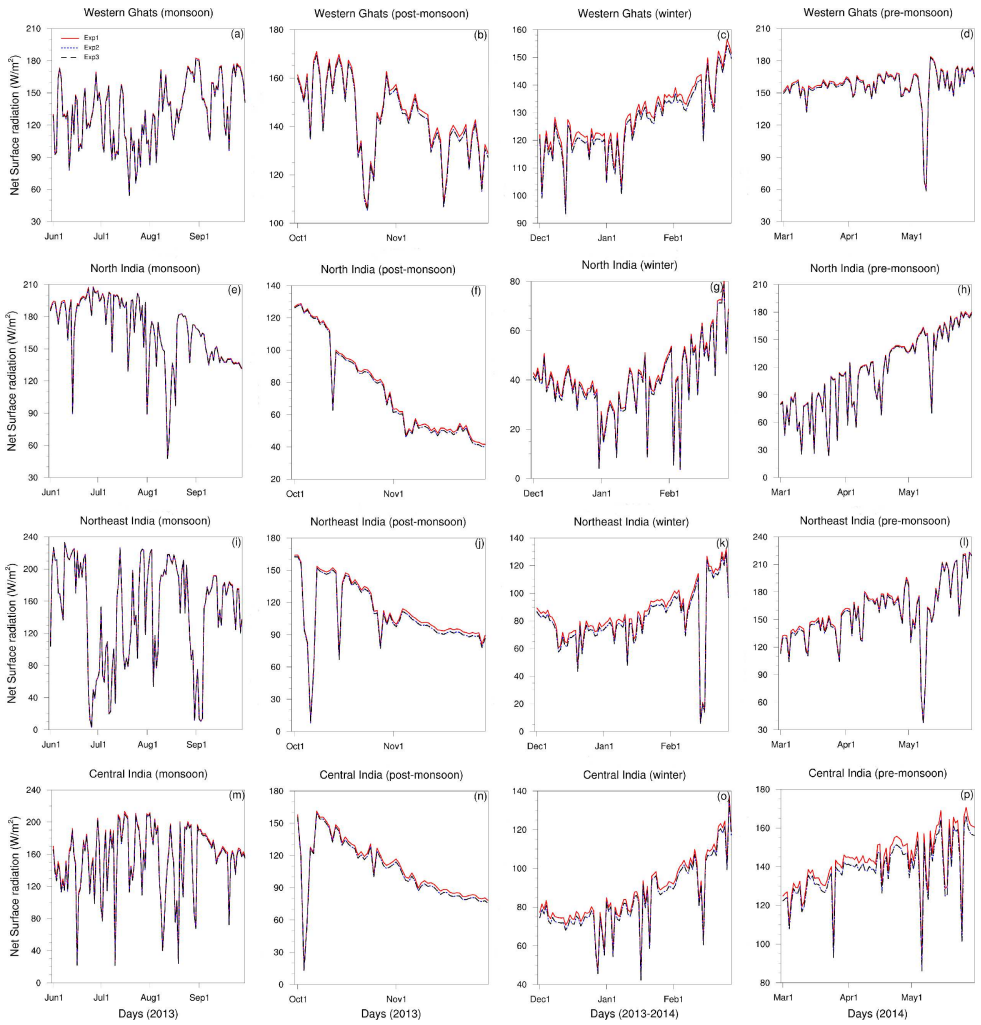

Fig. 11 Time series of daily mean Net Surface radiation spatially averaged over Central India, North India, Northeast India, and Western ghats for different seasons for all three experimental runs.

increased SM availability in Exp1-run as compared to Exp3-run. Additionally, the increased transpiration and canopy evaporation in the Exp1-run resulting from increased greenness fraction and the changes in land cover also contributes to an increase in LHF value for the Exp1-run. Furthermore, the conversion of cropland to forest land results in an increase of higher surface roughness, which increases the turbulent driven latent heat flux between the land surface and the atmosphere (Lee and Berbery, 2012). The change of LHF value between Exp1-run and Exp3-run in the seasonal mean of LHF is maximum for the post-monsoon season and winter season for all regions, while the minimum value of the difference of mean LHF between the Exp1-run and Exp3-run is attained in the monsoon season. The aforementioned observation can be explained by advancing the following argument. It is clear from Figure 4 that the difference of SM value between Exp1-run and Exp3-run are lowest during the monsoon season over all the four regions. Furthermore, the difference of SM value between Exp1-run and Exp3-run are highest during the post-monsoon season and winter season (refer Figure 4). It is clear that the latent heat flux will most definitely reflect the signature of the soil moisture. The increase in LHF for EXP1 compared to EXP3 is also attributed to the fact that the net surface radiation for the EXP1 is higher (refer to Figure 10)as compared to EXP3.

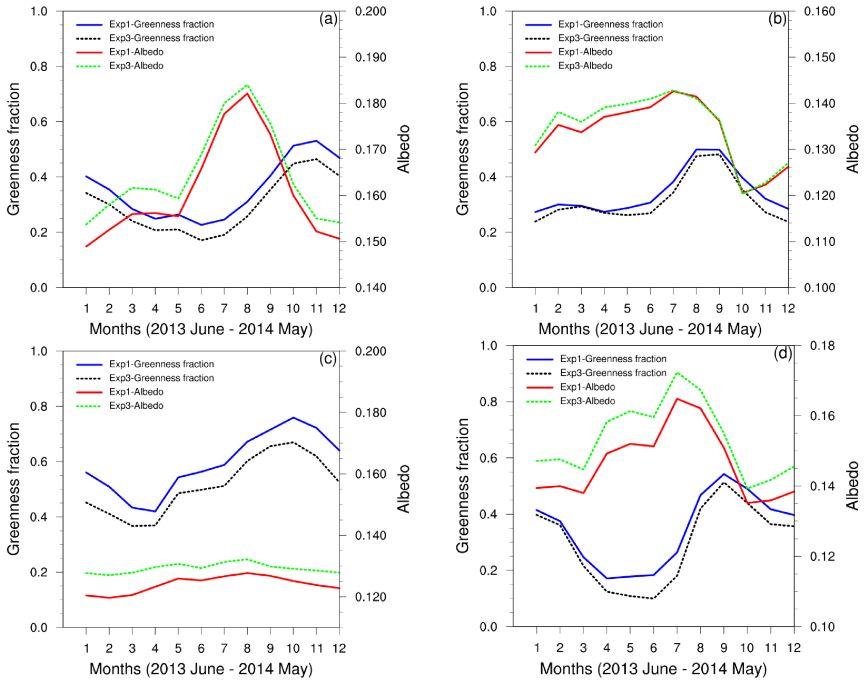

Fig. 12 Time series of monthly mean albedo and greenness fraction spatially averaged over Western ghats (a), North India (b), Northeast India (c), and Central India (d) for Exp1 run and Exp3 run, respectively.

Figure 10 shows a consistent daily mean increment in SHF for Exp3-run as compared to Exp3-run for all the regions and all the seasons. The reason for the above, is that for Exp3-run, the shrubs and grasses lands are incapable of liberating the same flux of moisture in the Exp3-run in the form of LHF as the forest cover. Due to the above reason, evaporative cooling decreases with an increase in the soil temperature, and SHF for the Exp3-run. In addition, the shallow-rooted vegetation, that cannot access water from deeper soil layers will experience a decrease in transpiration in Exp3-run and hence consequently an increase in SHF value for Exp3-run as compared to deep-rooted vegetation.

Figure 11 shows the time series of daily mean net surface radiation (NSR) spatially averaged over Central India, North India, Northeast India, and Western ghats for different seasons and for all the three experimental runs. Similar to the LHF and SHF, the NSR also shows lower values during the winter season as compared to the other three seasons and for all the four regions. The results of Figure 11 shows that the NSR value shows a decrease in Exp3-run as compared to Exp1-run. NSR typically depends on land surface albedo, net shortwave radiation, and outgoing longwave radiation. Figure 12 depicts the time series of monthly mean albedo and greenness fraction for Exp1-run and Exp3-run, that is spatially averaged over Western ghats (a), North India (b), Northeast India (c), and Central India (d). The spatial averaging in Figure 12 of the albedo and the greenness fraction over a region is averaged over all the grid points that encompass that region. It is clear from Figure 12 that the mean albedo and mean greenness fraction of Exp3-run is consistently lower as compared to the Exp1-run. The aforementioned observation is consistent with the present understanding of the land-atmosphere interaction processes. It is clear from Figure 12 that Exp3-run corresponds to higher albedo and higher outgoing long wave radiation (due to higher soil temperature) and hence it is clear that Exp1-run has consistently lower NSR values as compared to Exp3-run. It is clear from Figure 12 that for all the four regions, the albedo

Table 2 Summary of simulations

Simulation	Land cover	Soil texture		Albedo and Greenness fraction
Ctl-run	MODIS-IGBP	STATSGO-FAO		NCEP
Exp1-run	Potential land cover (1930)	Modified (1930)	STATSGO-FAO	modified NCEP (1930)
Exp2-run	Potential land cover (1975)	Modified (1975)	STATSGO-FAO	modified NCEP (1975)
Exp3-run	Potential land cover (2013)	Modified (2013)	STATSGO-FAO	modified NCEP (2013)

Table 3 The annual mean change of Latent heat flux, Sensible heat flux, Soil moisture, Soil temperature, and Net surface radiation due to historic land cover change (1930-2013) from forest (Evergreen needle leaf (ENL), Evergreen broadleaf (EBL), Decidious broadleaf (DBL), Mixed forest (MF)) to cropland, grassland, urbanland, and open shrub land respectively over Western ghats, North India, Northeast India and Central India. Student's t-test are performed and entries with 90% and 95% statistical significance level are indicated by (underlined) and (*), respectively.

Region	Landcover change	LHF(W/m^2)	SHF(W/m^2)	SM(m^3/m^3)	ST(K)	NSR(W/m^2)
Western Ghats	EBL to Crop	-26.55*	-14.79*	-0.06*	0.71	-11.87*
	EBL to Grass	-31.85*	<u>19.65</u>	-0.04	1.12	-11.23*
	EBL to Open shrub	-43.74*	24.06*	-0.02	<u>1.85</u>	-22.07*
North India	ENL to Crop	-16.29*	-1.62	0.05*	0.58	-7.72
	ENL to Open shrub	-23.06*	-0.54	0.07*	1.37	-13.05
	MF to Open shrub	-19.60*	14.51*	0.08*	1.46	-8.98
Northeast India	EBL to Crop	-25.57*	10.50	-0.07	0.85	-6.31
	EBL to Grass	-27.93*	17.55*	-0.05	1.12	-8.30
	EBL to Open shrub	35.83*	21.09*	-0.04	2.00	-22.53*
	ENL to Open shrub	-33.56*	15.10*	0.01	1.57	-23.55*
Central India	MF to Crop	-15.60	2.91	-0.02	0.76	-14.79

is maximum for both Exp1-run and Exp3-run during the July-August months. Since the Normalised difference vegetation index (NDVI) for wet evergreen forest and subtropical broadleaf forest over the Indian domain is minimum during the months July and August, the albedo peaks during the above months. Saritha P. K. (2017) studied the variability of land surface albedo associated with the different land cover types over the Indian domain. The study shows that most land cover types show peak albedo values during the Julian days 195-202.

4.4 Impact on land surface characteristics due to the change of different landcover classes over the Indian domain

Table 3 shows the impact of dominant land cover change (1930-2013) on land surface characteristics such as LHF, SHF, SM, ST and NSR over Western Ghats, North India, Northeast India, and Central India. The annual change of LHF, SHF, SM, ST and NSR depicted in Table 3 is only averaged over the grid points in a particular region where the above mentioned landcover change has been observed from the year 1930 to 2013, respectively. A two-tailed student's t-test is performed for corroborating

Table 4 The annual mean change of Latent heat flux, Sensible heat flux, Soil moisture, Soil temperature, and Net surface radiation due to historic land cover change (1930-2013) from forest (Evergreen needle leaf (ENL), Evergreen broadleaf (EBL), Decidious broadleaf (DBL), Mixed forest (MF)) to cropland, grassland, urbanland, and open shrub land respectively. Student's *t*-test are performed and entries with 90% and 95% statistical significance level are indicated by (underlined) and (*), respectively.

Variable	Forest type	Crop	Grass	Urban	Open shrub
Latent heat flux (W/m^2)	ENL	-16*	-19*	-66.83*	-25*
	EBL	-25.63*	-29.81*	-74.08*	-40.11*
	DBL	-17.43*	-21.38*	-57.19*	-31.05*
	MF	-13.52*	-15.08*	-62.44*	-23.29*
Sensible heat flux (W/m^2)	ENL	-11.71	9.46*	49.59*	13.92*
	EBL	-13.46*	16.69*	67.05*	21.21*
	DBL	-14.09	8.41*	44.51*	2.11
	MF	-17.11*	-17.13*	45.94*	-15.88*
Soil moisture (m^3/m^3)	ENL	0.06*	0.06*	0.13*	0.07*
	EBL	-0.06*	-0.05*	0.08*	-0.02
	DBL	-0.07*	-0.08	0.11*	-0.01
	MF	0.05*	0.06*	0.14*	0.07*
Soil temperature (K)	ENL	0.45	0.55	3.17	1.44
	EBL	0.76	1.07	2.85*	1.91
	DBL	0.36	0.65	2.67	1.51
	MF	0.53	0.59	2.93	1.42
Net surface heat flux (W/m^2)	ENL	-9.83*	-10.74*	-20.77*	-18.90*
	EBL	-11.52*	-11.02*	-13.81*	-21.49*
	DBL	-11*	-9.88*	-19.08*	-18.68*
	MF	-11.69*	-11.75*	-16.73*	-15.56*

the statistical significance of the results of Table 3. Entries in the Table 3 with '*' indicates 95% of statistical significance level, while the underlined entries indicate 90% of statistical significance level. From Table 3 it is clear that all landcover changes from forest (ENL, EBL, DBL and MF) to other landcover types such as cropland, grassland, urban and open shrubland, show a consistent reduction in latent heat flux values. Table 3 shows that the reduction is maximum for the land cover change from forest to open shrubland, followed by landcover change from forest to grassland and finally from forest to cropland. The above mentioned observation can be explained since the greenness fraction is lower in open shrubland as compared to cropland, and grassland, respectively. Furthermore, evapotranspiration values are lower for the open shrubland as compared to grassland and cropland, respectively. Over the Western ghats and Northeast India, the reduction in LHF is large for the landcover change from EBL forest to grassland as compared to landcover change from EBL forest to cropland. The reason for the above is that the deeper extended root depth and higher greenness fraction of cropland results in higher evapotranspiration for the cropland as compared to grassland. The above results are consistent with the earlier studies Duveiller et al. (2018). The statistically significant results show an increase in sensible heat flux when the forest land cover changes to other land cover types except for the cropland, which shows a decrease in sensible heat flux. Like the latent heat flux, the maximum change in sensible heat flux is also for the change from forest land cover to open shrubland followed by change from forest to grassland

and cropland, respectively. The above observation is easily explained since any decrease in latent heat flux leads to a corresponding increase in the sensible heat flux, by invoking the surface energy balance. Except for North India, all the other three regions show a decrease in soil moisture estimates when the land cover changes from forest to other land cover types. Over the Western Ghats, the largest change in soil moisture values for the land cover change from EBL to cropland has a value of -0.06 m^3/m^3 which is statistically significant at the 95% level. Over North India, the land cover changes from ENL to cropland, ENL to open shrubland, and MF to open shrubland show an increase in the soil moisture values. The above results for North India are at variance with the expected trend and is due to the nature of the soil texture of the corresponding land cover type observed over North India. All three land cover changes over North India from forest to other land cover types result in soil texture with higher porosity which contributes to increase in soil moisture. All land cover changes from forest to cropland, from forest to grassland, and from forest to open shrubland show an increase in soil temperature values. However, the changes in soil temperature are significant only for (up to 90% significant level) the land cover change from EBL forest to open shrubland over the Western ghats with a value of 1.85 K. The above feature is consistent with the fact that the maximum negative change in latent heat flux and maximum positive change in sensible heat flux also correspond to the land cover change from EBL to open shrubland. The NSR flux values show a consistent reduction for all land cover changes from forest to other land cover types. This is attributed to the higher albedo values of open shrubland as compared to the albedo values of grassland and cropland, respectively.

Annual mean change of surface fluxes (LHF and SHF) , SM, and soil temperature (ST) for the land cover changes from forest to crops, grassland, open shrubland, and urban land over the Indian domain due to historical land cover changes (1930-2013) are shown in Table 4. Table 4 is similar to Table 3 in the sense that the mean change of LHF, SHF, SM, ST and NSR are only averaged over the grid points over India when the above mentioned landcover changes has been observed from the year 1930 to 2013, respectively. Results from Table 4 indicate a consistent decrease in LHF values in all four cases. Since the cropland (CL), grassland (GL), open shrubland (OSL), and urban land (UL) have lower evapotranspiration values as compared to forest, the above is consistent with a decrease of LHF from forest to other landcover types (Kvalevåg et al., 2010). The annual mean change in LHF is highest for landcover change to UL compared to other land cover classes and is attributed to the low greenness fraction values and the limited impervious fraction of water over the UL. The evergreen broadleaf forest (EBF) has the largest change in the annual mean LHF as compared to other forest types. With EBL, the change in LHF is maximum for UL (-74.08 W/m^2) followed by OSL (-40.11 W/m^2), GL (-29.81 W/m^2) and CL (-25.63 W/m^2). The above is attributed to the high greenness fraction values and higher root depth of EBL forest compared to other forest types. Additionally, the evapotranspiration is higher for CL than GL due to the high greenness fraction and high root depth of CL as compared to GL. Table 4 reveals that the mean annual change in SHF is higher for all the land cover changes from forest to other landcover types except for the land cover change from forest to CL. It is to be noted that the magnitude of the decrease in sensible heat flux is lower than the magnitude of the decrease in the latent heat flux when there is a change from forest to cropland. The above does show that the effect on the latent heat flux change is more dominant as compared to the effect on the sensible heat flux change. The increase in SHF for the land cover change from EBF to GL is consistent with the results of Duveiller

et al. (2018). Similar to LHF, the annual mean change in SHF is highest for the land cover change from forest to UL compared to other landcover types and is due to the high albedo associated with UL as compared to the albedo values of GL and CL, respectively. Table 4 shows a consistent reduction in NSR values for all land cover changes from forest to CL, OSL, GL, and UL. Land cover change from forest to short vegetation over the tropics is generally associated with an increase in surface albedo, contributing to the decrease of NSR. The landcover change to OSL shows a large annual decrease in NSR values as compared to GL and CL types, respectively since the albedo values are higher for OSL as compared to the albedo value of GL and CL, respectively. The historical land cover change from forest to CL, GL, OSL, and UL contribute to increasing the soil temperature (ST). The deforestation studies of Kvalevåg et al. (2010) and Halder et al. (2016) over Indian domain also show an increase in surface temperature. The highest annual mean change of 2.85 K in ST is associated with the landcover change from EBL forest to UL, the above meeting the 95% statistical significance level. The above feature is attributed to the high greenness fraction of the EBL forest. Furthermore, the evaporative cooling is low over UL as compared to OSL, GL, and CL, respectively. Results of regional studies over the Indian domain also indicate that the urbanization scenario has contributed to an increase in the surface temperature (Li et al., 2017). The annual mean change in ST is significant for UL, followed by OSL, GL, and CL. This is because the canopy coverage can shade the soil surface, which lowers ST; the canopy coverage is more for the CL followed by GL and OSL. Conversion of EBL forest to open shrubland shows an increase in ST by 2.11 K with 90% of the statistical significance level. The land cover change for the forest type ENL and MF show an increase in soil moisture, when the land cover is changed to non-forest type. However, the EBL and DBL forest types show a decrease in soil moisture when the land cover is changed to non-forest type with the above meeting the 95% statistical significance level. Results indicate that the annual mean of latent heat flux and net surface heat flux reduced by -24.74 W/m^2 and -14.18 W/m^2 while the soil temperature and sensible heat flux increased by 2.78 K and 4.97 W/m^2,respectively.

5 Conclusion

The present study utilized the Noah LSM to study the impacts of historical land cover changes on land surface characteristics from 1930-2013. Four simulations are performed using Noah LSM, (i) Ctl-run, and (ii) to (iv) the three Experiment runs. Ctl-run is simulated using MODIS-IGBP land cover, NCEP albedo, and NCEP greenness fraction data, while the three experimental runs are simulated using three different potential land cover maps (1930, 1975, and 2013), and associated with modified albedo, and modified greenness fraction data. For the analysis, four regions are selected, where the land cover changes are clearly discernable, namely, Western ghats, North India, Central India, and Northeast India.

Results indicate that land cover change (1930 to 2013) reduces latent heat flux and net surface radiation in all the four regions and for all the seasons. The above behavior can be explained by invoking the decrease of evapotranspiration and the increase of albedo in all the four regions for the Exp-3 run. The land cover change from forest to other land cover types resulted in increased sensible heat flux and soil temperature for all four regions and for all the seasons. This is attributed to the fact that reduced latent heat flux results in Exp-3 run contributing to an increase in the sensible heat flux by invoking the surface energy balance. Also, the reduced greenness fraction due to land cover change from forest to

other land cover types can increase the amount of radiation that reaches the land surface, resulting in the surface warming effect. The land cover change from forest to other land cover types decreases the soil moisture for all regions except for North India, where the soil moisture estimate increases and shows a different behavior. Results show that the maximum annual mean change in latent heat flux and net surface radiation is for the land cover change from the forest (EBL, ENL, MF) to open shrubland as compared to forest to grassland and forest to cropland, due to low evapotranspiration and high albedo for open shrubland type as compared to grassland and cropland types. The soil temperature increases for all land cover changes from forest to other land cover types for all regions; however, the land cover change from EBL to open shrubland over Western ghats shows the highest increase in soil temperature having a value of 1.85 K, the above meeting the 90% statistical significance level. Over North India, the soil moisture estimates increases due to land cover change from forest to other land cover types, which is attributed to the soil texture of the corresponding land cover class over North India. The results are consistent with regional results. Over the Indian domain, the maximum change in latent heat flux and sensible heat flux correspond to the land cover change from forest to urban land as compared to the forest to cropland, forest to open shrubland, and forest to grassland. Land cover change from EBL to urban land shows the maximum decrease in latent heat flux (-74.08 W/m^2) and maximum increase in sensible heat flux (67.05 W/m^2), both meeting the 95% of the statistical significance level. Results indicate that the annual mean of latent heat flux and net surface radiation is reduced by -24.74 W/m^2 and -14.18 W/m^2, while the sensible heat flux and soil temperature increases by 4.97 W/m^2 and 2.78 K.

ACKNOWLEDGEMENTS

The authors thank the Hydrological Sciences Laboratory at NASA's Goddard Space Flight Center (GSFC) for providing the LIS (Land Information System). The Research Application Laboratory (RAL), National Center for Atmospheric Research (NCAR), USA is acknowledged for providing the 1D Noah LSM. The authors acknowledge the National Remote Sensing Centre, Indian Space Research Organization (ISRO) for providing the fractional forest cover data. The first author (Vibin Jose) also thanks the Council of Science and Industrial Research (CSIR), Government of India for providing Research Fellowship. The authors also gratefully acknowledge the Director of IIST (Indian Institute of Space Science and Technology) for the support, encouragement and for providing the High-Performance Computing (HPC) facility. The authors acknowledge the comments received from the two anonymous reviewers, which have improved the manuscript.

Conflicts of Interest

The authors declare no conflict of interest.

Funding

The present study has not received any specific grant or funding from any agency.

Author's Contributions

While the second author assisted in the design of the study and contributed to interpretation and broad conclusion of the results, the first author contributed in carrying out the detailed model simulations, as well as additional analysis that were carried out. Furthermore, the first author contributed to writing the manuscript.

Availability of data and material

The data sets and material used in the present study are freely available in the web.

Code availability

The codes employed in this study are available to be shared on request.

Ethics approval

The authors declare that the contents and the results of the manuscript have not been published in any other journal or conference.

Consent to participate and Consent for publication

The authors provide their consent and willingness to participate in the publication process and to publish the above manuscript.

Disclosure statement

No conflict of interest is reported by the authors.

References

Anyanwu C (2015) The impact of deforestation on soil conditions in anambra state of nigeria. Agriculture, Forestry and Fisheries 4:64, DOI 10.11648/j.aff.s.2015040301.21

Betts R (2001) Biogeophysical impacts of land use on present-day climate: Near-surface temperature and radiative forcing. Atmospheric Science Letters 2:39 – 51, DOI 10.1006/asle.2001.0037

Betts R, Falloon P, Klein Goldewijk K, Ramankutty N (2007) Biogeophysical effects of land use on climate: Model simulations of radiative forcing and large-scale temperature change. Agricultural and Forest Meteorology 142:216–233, DOI 10.1016/j.agrformet.2006.08.021

Bonan G (2008) Forests and climate change: Forcings, feedbacks, and the climate benefits of forests. Science (New York, NY) 320:1444–1449, DOI 10.1126/science.1155121

Bounoua L, Defries R, Collatz G, Sellers P, Khan H (2002) Effects of land cover conversion on surface climate. cc 52:29–, DOI 10.1023/A:1013051420309

Bright R, Davin E, O'Halloran T, Pongratz J, Cescatti A (2017) Local temperature response to land cover and management change driven by non-radiative processes. Nature Climate Change 7:296–302, DOI 10.1038/nclimate3250

Case KMLCJASWML J L, Peters-Lidard CD (2007) Improved modelling of land-atmosphere interactions using a coupled version of wrf with the land information system

Chase T (1999) The role of historical land-cover changes as a mechanism for global and regional climate change. PhD thesis, Colorado State University

Chase T, Pielke Sr R, Kittel T, Nemani R, Running S (2000) Simulated impacts of historical land cover changes on global climate in northern winter. Climate Dynamics 16:93–105, DOI 10.1007/s003820050007

Chen F, Mitchell K, Schaake J, Xue Y, Pan HL, Koren V, Duan QY, Ek M, Betts A (1996) Modeling of land surface evaporation by four schemes and comparison with fife observations. Journal of Geophysical Research: Atmospheres 101(D3):7251–7268

Cherubini F, Huang B, Hu X, Tölle M, Strømman A (2018) Quantifying the climate response to extreme land cover changes in europe with a regional model. Environmental Research Letters 13, DOI 10.1088/1748-9326/aac794

Csiszar I, Gutman G (1999) Mapping global land surface albedo from noaa avhrr. Journal of Geophysical Research 104:6215–6228, DOI 10.1029/1998JD200090

Davin E, de NOBLET N (2010) Climatic impact of global-scale deforestation: Radiative versus nonradiative processes. Journal of Climate - J CLIMATE 23, DOI 10.1175/2009JCLI3102.1

Deng X, Zhao C, Yan H (2013) Systematic modeling of impacts of land use and land cover changes on regional climate: A review. Advances in Meteorology 2013, DOI 10.1155/2013/317678

Dirmeyer AP, Niyogi D, Noblet-Ducoudre ND, Dickinson RE, Snyder PK (2010) Impacts of land use change on climate. International Journal of climatology 30:1905–1907

Dirmeyer PA, Halder S (2016) Sensitivity of numerical weather forecasts to initial soil moisture variations in cfsv2. Weather and Forecasting 31(6):1973–1983

Dong N, Liu Z, Luo M, Fang C, Lin H (2019) The effects of anthropogenic land use changes on climate in china driven by global socioeconomic and emission scenarios. Earth's Future 7(7):784–804, DOI https://doi.org/10.1029/2018EF000932

Dutta S, Das S, Kar S, Mohanty UC, Joshi P (2009) Impact of vegetation on the simulation of seasonal monsoon rainfall over the indian subcontinent using a regional model. Journal of Earth System Science 118, DOI 10.1007/s12040-009-0048-z

Duveiller G, Hooker J, Cescatti A (2018) The mark of vegetation change on earth's surface energy balance. Nature Communications 9, DOI 10.1038/s41467-017-02810-8

Feddema J, Oleson K, Bonan G, Mearns L, Washington W, Meehl G, Nychka D (2005) A comparison of a gcm response to historical anthropogenic land cover change and model sensitivity to uncertainty in present-day land cover representations. Climate Dynamics 25:581–609, DOI 10.1007/s00382-005-0038-z

Findell KL, Knutson TR, Milly PCD (2006) Weak simulated extratropical responses to complete tropical deforestation. Journal of Climate 19(12):2835 – 2850, DOI 10.1175/JCLI3737.1, URL `https://journals.ametsoc.org/view/journals/clim/19/12/jcli3737.1.xml`

693 Friedl M, McIVer D, Hodges J, Zhang X, Muchoney D, Strahler A, Woodcock C, Gopal S, Schneider
694 A, Cooper A, Baccini A, Gao F, Schaaf C (2002) Global land cover mapping from modis: Algorithms
695 and early results. Remote Sensing of Environment 83:287, DOI 10.1016/S0034-4257(02)00078-0
696 Garratt J (1993) Sensitivity of climate simulations to land-surface and atmospheric boundary-layer
697 treatments-a review. Journal of Climate; (United States) 6:3, DOI 10.1175/1520-0442(1993)006⟨0419:
698 SOCSTL⟩2.0.CO;2
699 Gogoi P, Vinoj V, Swain D, Roberts G, Dash J, Tripathy S (2019) Land use and land cover change effect
700 on surface temperature over eastern india. Scientific Reports 9, DOI 10.1038/s41598-019-45213-z
701 Gruber A, Dorigo W, Crow W, Wagner W (2017) Triple collocation-based merging of satellite soil
702 moisture retrievals. IEEE Transactions on Geoscience and Remote Sensing PP:1–13, DOI 10.1109/
703 TGRS.2017.2734070
704 Guo W, Wang X, Sun J, Ding A, Jun Z (2016) Comparison of land–atmosphere interaction at different
705 surface types in the mid- to lower reaches of the yangtze river valley. Atmospheric Chemistry and
706 Physics 16:9875–9890, DOI 10.5194/acp-16-9875-2016
707 Gutman G, Ignatov A (1998) The derivation of the green vegetation fraction from noaa/avhrr data
708 for use in numerical weather prediction models. International Journal of Remote Sensing 19, DOI
709 10.1080/014311698215333
710 Halder S, Saha S, Dirmeyer P, Chase T, Goswami BN (2016) Investigating the impact of land-use
711 land-cover change on indian summer monsoon daily rainfall and temperature during 1951–2005 us-
712 ing a regional climate model. Hydrology and Earth System Sciences 20:1765–1784, DOI 10.5194/
713 hess-20-1765-2016
714 Hansen J, Sato M, Ruedy R, Nazarenko L, Lacis A, Schmidt G, Russell G, Aleinov I, Bauer M, Bauer
715 S, Bell N, Cairns B, Canuto V, Chandler M, Cheng Y, Delgenio A, Faluvegi G, Fleming E, Friend
716 A, Zhang S (2005) Efficacy of climate forcings. Journal of Geophysical Research 110, DOI 10.1029/
717 2005JD005776
718 Huang H, Xue Y, Chilukoti N, Liu Y, Chen G, Diallo I (2020) Assessing global and regional ef-
719 fects of reconstructed land-use and land-cover change on climate since 1950 using a coupled
720 land–atmosphere–ocean model. Journal of Climate DOI 10.1175/JCLI-D-20-0108.1
721 Jose V, Chandrasekar A (2021) Impacts of different rainfall forcings on soil moisture distribution
722 over india: Assessment using the land information system. Pure Appl Geophys 178, DOI 10.1007/
723 s00024-021-02798-9
724 Kolassa J, Gentine P, Prigent C, Aires F, Alemohammad S (2017) Soil moisture retrieval from AMSR-E
725 and ASCAT microwave observation synergy. part 2: Product evaluation. Remote Sensing of Environ-
726 ment 195:202–217, DOI 10.1016/j.rse.2017.04.020
727 Kumar S, Peters-Lidard C, Tian Y, Houser P, Geiger J, Olden S, Lighty L, Eastman J, Doty B, Dirmeyer
728 P, Adams J, Mitchell K, Wood E, Sheffield J (2006) Land information system: An interoperable
729 framework for high resolution land surface modeling. Environmental Modelling & Software 21(10):1402
730 – 1415, DOI https://doi.org/10.1016/j.envsoft.2005.07.004
731 Kvalevåg M, Myhre G, Bonan G, Levis S (2010) Anthropogenic land cover changes in a gcm with
732 surface albedo changes based on modis data. International Journal of Climatology 30:2105 – 2117,
733 DOI 10.1002/joc.2012

734 Lawrence P, Chase T (2010) Investigating the climate impacts of global land cover change in the commu-
735 nity climate system model. International Journal of Climatology 30:2066 – 2087, DOI 10.1002/joc.2061
736 Lee SJ, Berbery E (2012) Land cover change effects on the climate of the la plata basin. Journal of
737 Hydrometeorology 13:84–102, DOI 10.1175/JHM-D-11-021.1
738 Li X, Mitra C, Dong L, Yang Q (2017) Understanding land use change impacts on microclimate using
739 weather research and forecasting (wrf) model. Physics and Chemistry of the Earth, Parts A/B/C 103,
740 DOI 10.1016/j.pce.2017.01.017
741 Liu F, Tao F, Liu J, Zhang S, Xiao D, Wang M, Zhang H, Huizi B (2014) Effects of land use/cover
742 change on land surface energy partitioning and climate in northeast china. Theoretical and Applied
743 Climatology 123, DOI 10.1007/s00704-014-1340-7
744 Liu Y, Guo W, Song Y (2015) Estimation of key surface parameters in semi-arid region and their
745 impacts on improvement of surface fluxes simulation. Science China Earth Sciences 59, DOI 10.1007/
746 s11430-015-5140-4
747 Liu Y, Xue Y, MacDonald G, Cox P, Zhang Z (2019) Global vegetation variability and its response to
748 elevated co¡sub¿2¡/sub¿, global warming, and climate variability – a study using the offline ssib4/triffid
749 model and satellite data. Earth System Dynamics 10:9–29, DOI 10.5194/esd-10-9-2019
750 Lozano-Parra J, Pulido M, Lozano C, Schnabel S (2018) How do soil moisture and vegetation covers influ-
751 ence soil temperature in drylands of mediterranean regions? Water 10:1747, DOI 10.3390/w10121747
752 McColl KA, Vogelzang J, Konings AG, Entekhabi D, Piles M, Stoffelen A (2014) Extended triple collo-
753 cation: Estimating errors and correlation coefficients with respect to an unknown target. Geophysical
754 Research Letters 41(17):6229–6236, DOI 10.1002/2014GL061322
755 Miller DA, White RA (1998) A conterminous united states multilayer soil characteristics dataset for
756 regional climate and hydrology modeling. Earth Interactions 2(2):1 – 26, DOI 10.1175/1087-3562(1998)
757 002⟨0001:ACUSMS⟩2.3.CO;2
758 Mishra V, Cherkauer K, Niyogi D, Lei M, Pijanowski B, Ray D, Bowling L, Yang G (2010) A regional
759 scale assessment of land use/land cover and climatic changes on water and energy cycle in the upper
760 midwest united states. International Journal of Climatology 30:2025 – 2044, DOI 10.1002/joc.2095
761 Nair A, Indu J (2019) Improvement of land surface model simulations over india via data assimilation
762 of satellite-based soil moisture products. Journal of Hydrology 573:406–421, DOI 10.1016/j.jhydrol.
763 2019.03.088
764 Nair U, Wu Y, Kala J, Lyons T, Pielke Sr R, Hacker J (2011) The role of land use change on the
765 development and evolution of the west coast trough, convective clouds, and precipitation in southwest
766 australia. Journal of Geophysical Research 116, DOI 10.1029/2010JD014950
767 Niu C, Musa A, Liu Y (2015) Analysis of soil moisture condition under different land uses in the arid
768 region of horqin sandy land, northern china. Solid Earth 6, DOI 10.5194/se-6-1157-2015
769 Niyogi D, Kishtawal C, Tripathi S, Govindaraju R (2010) Observational evidence that agricultural
770 intensification and land use change may be reducing the indian summer monsoon rainfall. Water
771 Resources Research - WATER RESOUR RES 46, DOI 10.1029/2008WR007082
772 Niyogi D, Mohanty UC, Kishtawal C, Ghosh S, Nair U, Ek M, Rajeevan M (2018) The Impact of
773 Land Cover and Land Use Change on the Indian Monsoon Region Hydroclimate, pp 553–575. DOI
774 10.1007/978-3-319-67474-2_25

Oleson K, Bonan G, Levis S, Vertenstein M (2004) Effects of land use change on north american climate: Impact of surface datasets and model biogeophysics. Climate Dynamics 23:117–132, DOI 10.1007/s00382-004-0426-9

Pai D, Sridhar L, Rajeevan M, Sreejith OP, Satbhai N, Mukhopadhyay B (2014) Development of a new high spatial resolution (0.25° × 0.25°) long period (1901-2010) daily gridded rainfall data set over india and its comparison with existing data sets over the region. Mausam 65:1–18

Peng S, Piao S, Zeng Z, Ciais P, Zhou L, Li L, Myneni R, Yin Y, Zeng H (2014) Afforestation in china cools local land surface temperature. Proceedings of the National Academy of Sciences of the United States of America 111, DOI 10.1073/pnas.1315126111

Pielke RA, Avissar R, Raupach M, Dolman AJ, Zeng X, Denning AS (1998) Interactions between the atmosphere and terrestrial ecosystems: influence on weather and climate. Global Change Biology 4(5):461–475, DOI https://doi.org/10.1046/j.1365-2486.1998.t01-1-00176.x

Pielke RA, Pitman A, Niyogi D, Mahmood R, Mcalpine C, Hossain F, Klein Goldewijk K, Nair U, Betts R, Fall S, Reichstein M, Kabat P, de NOBLET N (2011) Land use/land cover changes and climate: Modeling analysis and observational evidence. Wiley Interdisciplinary Reviews: Climate Change 2:828 – 850, DOI 10.1002/wcc.144

Pitman A, de NOBLET N, Avila F, Alexander L, Boisier JP, Brovkin V, Delire C, Cruz F, Donat M, Gayler V, Hurk B, Reick C, Voldoire A (2012) Effects of land cover change on temperature and rainfall extremes in multi-model ensemble simulations. Earth System Dynamics 3:213–231, DOI 10.5194/esd-3-213-2012

Pitman AJ (2003) The evolution of, and revolution in, land surface schemes designed for climate models. International Journal of Climatology 23(5):479–510, DOI https://doi.org/10.1002/joc.893

Ramankutty N, Foley JA (1999) Estimating historical changes in global land cover: Croplands from 1700 to 1992. Global Biogeochemical Cycles 13(4):997–1027, DOI https://doi.org/10.1029/1999GB900046

Reddy CS, Saranya K, Shaik V, Satish K, Jha C, Diwakar P, Dadhwal V, Rao P, Murthy Y (2018) Assessment and monitoring of deforestation and forest fragmentation in south asia since the 1930s. Global and Planetary Change 161:132–148, DOI 10.1016/j.gloplacha.2017.10.007

Reynolds CA, Jackson TJ, Rawls WJ (2000) Estimating soil water-holding capacities by linking the food and agriculture organization soil map of the world with global pedon databases and continuous pedotransfer functions. Water Resources Research 36(12):3653–3662, DOI https://doi.org/10.1029/2000WR900130

Rodell M, Houser PR, Jambor U, Gottschalck J, Mitchell K, Meng CJ, Arsenault K, Cosgrove B, Radakovich J, Bosilovich M, Entin JK, Walker JP, Lohmann D, Toll D (2004) The global land data assimilation system. Bulletin of the American Meteorological Society 85(3):381–394, DOI 10.1175/BAMS-85-3-381

Rodell M, Houser PR, Berg AA, Famiglietti JS (2005) Evaluation of 10 methods for initializing a land surface model. Journal of Hydrometeorology 6(2):146–155, DOI 10.1175/JHM414.1

Sampaio G, Nobre C, Costa M, Satyamurty P, Filho B, Cardoso M (2007) Regional climate change over eastern amazonia caused by pasture and soybean cropland expansion. Geophysical Research Letters - GEOPHYS RES LETT 34, DOI 10.1029/2007GL030612

Saritha P K ARNRCVGB Keerthi V (2017) Variability analysis of land surface albedo associated with different land cover types in india

Sellers P, Hall F, Asrar G, Strebel D, Murphy R (1988) The first islscp field experiment (fife). B Am Meteorol Soc 69, DOI 10.1175/1520-0477(1988)069⟨0022:TFIFE⟩2.0.CO;2

Stoffelen A (1998) Toward the true near-surface wind speed: Error modeling and calibration using triple collocation. Journal of Geophysical Research: Oceans 103(C4):7755–7766, DOI 10.1029/97JC03180

Tyagi J, Qazi N, Rai SP, Singh M (2013) Analysis of soil moisture variation by forest cover structure in lower western himalayas, india. Journal of Forestry Research 24, DOI 10.1007/s11676-013-0355-8

van Zyl JJ (2001) The shuttle radar topography mission (srtm): a breakthrough in remote sensing of topography. Acta Astronautica 48(5):559–565, DOI https://doi.org/10.1016/S0094-5765(01)00020-0, URL https://www.sciencedirect.com/science/article/pii/S0094576501000200

Wu X, Lu G, Wu Z, He H, Scanlon T, Dorigo W (2020) Triple collocation-based assessment of satellite soil moisture products with in situ measurements in china: Understanding the error sources. Remote Sensing 12(14), DOI 10.3390/rs12142275

Zobler L, for Space Studies GI (1986) A World Soil File for Global Climate Modeling. NASA technical memorandum, National Aeronautics and Space Administration, Goddard Space Flight Center, Institute for Space Studies, URL https://books.google.co.in/books?id=iMQ9ygAACAAJ